Intermediate-energy differential and integral cross sections for vibrational excitation in α-tetrahydrofurfuryl alcohol

H. V. Duque, L. Chiari, D. B. Jones, Z. Pettifer, G. B. da Silva, P. Limão-Vieira, F. Blanco, G. García, R. D. White , M. C. A. Lopes, and M. J. Brunger

Citation: The Journal of Chemical Physics **140**, 214306 (2014); doi: 10.1063/1.4879779
View online: http://dx.doi.org/10.1063/1.4879779
View Table of Contents: http://scitation.aip.org/content/aip/journal/jcp/140/21?ver=pdfcov
Published by the AIP Publishing

Intermediate-energy differential and integral cross sections for vibrational excitation in α-tetrahydrofurfuryl alcohol

H. V. Duque,[1,2] L. Chiari,[1] D. B. Jones,[1] Z. Pettifer,[1] G. B. da Silva,[1,3] P. Limão-Vieira,[4] F. Blanco,[5] G. García,[6] R. D. White,[7] M. C. A. Lopes,[2] and M. J. Brunger[1,8,a)]

[1]*School of Chemical and Physical Sciences, Flinders University, GPO Box 2100, Adelaide, SA 5001, Australia*
[2]*Departamento de Física, Universidade Federal de Juiz de Fora, Juiz de Fora, MG, Brazil*
[3]*Universidade Federal de Mato Grosso, Barra do Garças, Mato Grosso, Brazil*
[4]*Laboratório de Colisões Atómicas e Moleculares, CEFITEC, Departamento de Física, Faculdade de Ciências e Tecnologia, Universidade Nova de Lisboa, 2829-516 Caparica, Portugal*
[5]*Departamento de Física Atómica, Molecular y Nuclear, Universidad Complutense de Madrid, Madrid E-28040, Spain*
[6]*Instituto de Física Fundamental, CSIC, Madrid E-28006, Spain*
[7]*School of Engineering and Physical Sciences, James Cook University, Townsville, 4810 Queensland, Australia*
[8]*Institute of Mathematical Sciences, University of Malaya, Kuala Lumpur, Malaysia*

(Received 22 April 2014; accepted 14 May 2014; published online 3 June 2014)

Differential and integral cross section measurements, for incident electron energies in the 20–50 eV range, are reported for excitation of several composite vibrational modes in α-tetrahydrofurfuryl alcohol (THFA). Optimisation and frequency calculations, using GAUSSIAN 09 at the B3LYP/aug-cc-pVDZ level, were also undertaken for the two most abundant conformers of THFA, with results being reported for their respective mode classifications and excitation energies. Those calculations assisted us in the experimental assignments of the composite features observed in our measured energy loss spectra. There are, to the best of our knowledge, no other experimental or theoretical data currently available in the literature against which we can compare the present results. © *2014 AIP Publishing LLC*. [http://dx.doi.org/10.1063/1.4879779]

I. INTRODUCTION

Low- and intermediate-energy electron scattering data are now available for a relatively large number of molecular targets, although in the vast majority of those cases that data are often incomplete.[1,2] While integral cross sections (ICSs) and differential cross sections (DCSs) have been calculated and measured with a wide variety of approaches, such data are typically only available for the elastic scattering channel. On the other hand, vibrational mode and electronic-state excitation cross sections are relatively scarce with this being true for both theoretical and experimental results. Unfortunately, it is precisely those inelastic cross sections, along with cross sections for dissociative electron attachment and ionisation, that are fundamental to obtaining a quantitative understanding of the role of electron-driven processes in many natural phenomena[3] and in technological (e.g., discharges and low-temperature plasmas)[4,5] and medical (e.g., simulating charged-particle tracks in matter)[6–8] applications. In the case of vibrational excitation, the work that has been done is usually associated with energy regimes where resonance enhancement, due to the temporary capture of the incident electron by the target, of the cross sections is found. While this is clearly very important, for example, in the understanding of infrared auroral emissions from NO molecules in our atmosphere,[9] because the magnitudes of those vibrational cross sections are significant when resonantly enhanced, there are also cases where cross section data away from resonance, e.g., at intermediate energies, although much smaller in magnitude, are still needed to quantitatively describe the phenomenon in question.[5,8,10]

α-tetrahydrofurfuryl alcohol (THFA), see Fig. 1, has recently been identified[11,12] as a better analogue moiety for the backbone sugar deoxyribose, than is the chemically similar species tetrahydrofuran (THF). However, significantly less experimental and theoretical effort has been devoted to THFA compared to THF.[5,10,13] The scattering data for THFA that is presently available in the literature (electron, positron, and photon) includes some independent atom method (IAM) elastic cross sections and binary-encounter Bethe (BEB) total ionisation cross sections,[14] a total cross section (TCS) measurement from Możejko *et al.*,[15] some elastic DCS data[16] at intermediate to high energies, a dissociative ionisation study from Milosavljević *et al.*,[17] and some dynamical (e,2e) investigations from Bellm *et al.*[18] and Jones *et al.*[19] More recently, a detailed study into electronic-state electron impact excitation (20–50 eV) in THFA has been advanced by Duque *et al.*[12] and Chiari *et al.*[20] We note that those latest investigations[12,20] also included IAM with screened additivity rule (SCAR) correction computations for elastic DCS and ICS and the TCS in THFA. From a positron perspective, we only know of the TCS measurement from Zecca *et al.*[21] Photoionisation cross sections are also available,[11,22] as are photoabsorption cross sections from the very recent measurement of Limão-Vieira *et al.*[11] That latter paper also contains a set of comprehensive electronic-structure calculations, which showed that of the six

a)Electronic mail: Michael.Brunger@flinders.edu.au

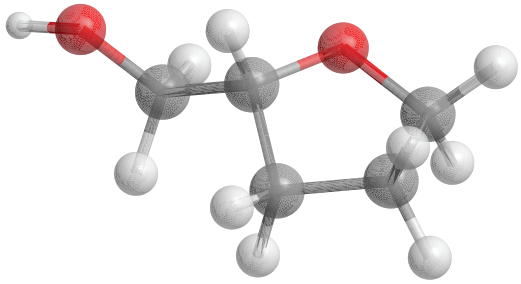

FIG. 1. Schematic diagram of the THFA molecule generated using ChemBio3D Ultra 2010 Suite.[46] The H, C and O atoms are indicated in white, grey and red, respectively.

lowest energy THFA conformers only four would be likely to be present in our THFA beam and of those conformers A and C would be predominant (~75% of the population).[11] The apparent lack of any electron impact vibrational excitation cross section data for THFA forms one important rationale for this investigation.

From a more fundamental perspective, α-tetrahydrofurfuryl alcohol possesses both a significant average dipole polarisability (~70.18 a.u.[12,23]) and strong permanent dipole moment (~2 D[12,15]) which have been previously observed[24–26] to have an important effect on the collision dynamics of other systems. Indeed Chiari *et al.*[20] found that the DCSs for excitation of Rydberg bands of electronic-states in THFA were all strongly peaked in magnitude at more forward electron scattering angles, a result indicative for the important dipole influence on the scattering process. However, in their recent measurements for vibrational excitation in THF, another polar species with a significant dipole polarisability, Khakoo *et al.*[27] found that the DCSs for the various excited modes, and over quite a wide energy range (~3–20 eV), were almost isotropic. That result suggests that the intrinsic molecular dipole properties of THF are not having a major effect on the vibrational excitation collision dynamics, an observation somewhat at odds with the electronic-state THF data of Do *et al.*[28] whose DCSs are all strongly peaked in magnitude at forward angles. Hence, another rationale for the current work was to study if the dipole moment and dipole polarisability of THFA do influence the electron impact vibrational excitation cross sections of this molecule. Details of our experimental method and analysis procedures are given in Sec. II, with our results and a discussion of those results then being presented in Sec. III. Finally, in Sec. IV, some concluding remarks will be drawn.

II. EXPERIMENTAL DETAILS AND ANALYSIS PROCEDURES

Examples of the electron energy loss spectra (EELS), measured in this study, are given in Fig. 2. Those data were acquired with an apparatus based at Flinders University,[29] which has been described in detail many times previously. Briefly, a monochromated beam of electrons with energies (E_0) in the range 20–50 eV and a typical flux of 1–3 nA was incident on an orthogonal beam of THFA. Our processes for ensuring a stable beam of THFA (Sigma-Aldrich, 99% assay)

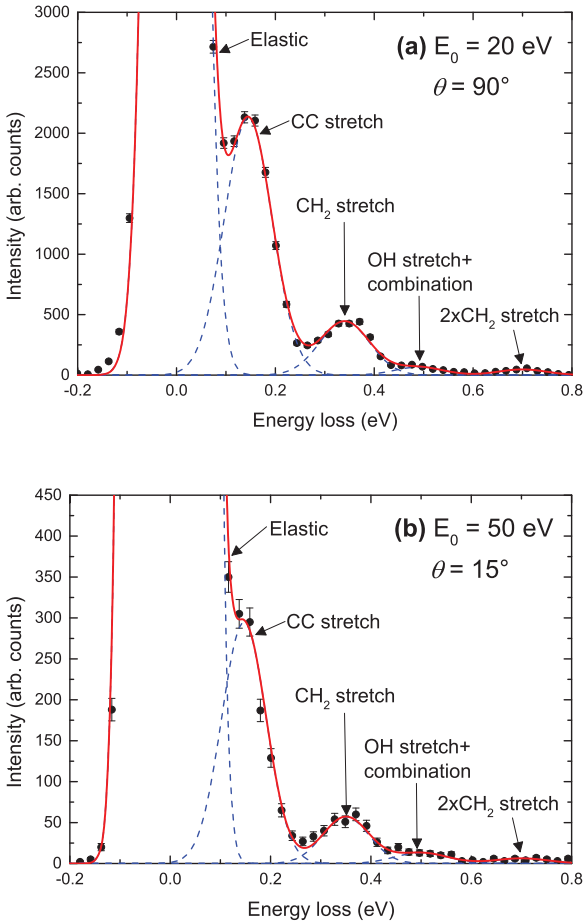

FIG. 2. Typical electron energy loss spectra of THFA at (a) $E_0 = 20$ eV, $\theta = 90°$ and (b) $E_0 = 50$ eV, $\theta = 15°$ over the range −0.2 to 0.8 eV. The overall spectral deconvolution fit is denoted by the solid red line, while the fits to the various vibrational features are also shown by the dashed blue lines. The features are identified according to their prevalent modes. For clarity the elastic peak has been truncated in each case.

into the interaction region were given in Duque *et al.*,[12] and so are not repeated here. Note that under the stable beam conditions maintained during the EELS measurements, the THFA pressure in the vacuum chamber was kept between $5–10\times10^{-6}$ Torr in order to minimise multiple scattering effects. The intersection of the electron and THFA beams defined a collision volume, and those electrons which collided with the molecules and scattered at some angle θ, known as the electron scattering angle, were energy analysed using a hemispherical selector before being detected with a channel electron multiplier. Note that the angular range of the present EELS was 10°–90°. Further note that the overall instrumental energy resolution employed in our measurements was ~65 meV (FWHM), which was insufficient to resolve many of the vibrational modes from one another (see Table I). As a consequence, composite vibrational mode cross sections are reported here (see Fig. 2). EELS were accumulated at each scattering angle and incident energy (20, 30, 40, and 50 eV) by recording the number of scattered electrons detected at each energy loss value. The true electron count rate at each given energy loss was recorded using a multichannel scaler (MCS) synchronised to a linear voltage ramp that varied the

TABLE I. Calculated vibrational energies (eV) of the most abundant conformers of THFA.[11] These values are used to assign the experimentally observed spectral features (see Fig. 2). Note that THFA has C_1 symmetry in its ground ($X\ ^1A$) electronic state.[11]

		Conformer A		Conformer C		
Experimental energy loss (eV)	Experimental assignment	Vib. mode	Energy (eV)	Vib. mode	Energy (eV)	Assignment
0	"Elastic"					Elastic peak
		ν_6	0.051	ν_6	0.050	OH rotation[a]
0.09–0.27	"CC stretch"	$2\times\nu_6$	0.102	$2\times\nu_6$	0.100	$2\times$ OH rotation
		ν_{15}	0.118	ν_{15}	0.119	
		ν_{17}	0.125	ν_{17}	0.125	CC stretch
		ν_{18}	0.129	ν_{18}	0.129	
		ν_{19}	0.133	ν_{19}	0.133	
		ν_{30}	0.168			COH bend
		ν_{31}	0.170	ν_{31}	0.170	
		$2\times\nu_{18}$	0.258	$2\times\nu_{18}$	0.258	
		$\nu_{18}+\nu_{19}$	0.262	$\nu_{18}+\nu_{19}$	0.262	$2\times$ CC stretch
		$2\times\nu_{19}$	0.266	$2\times\nu_{19}$	0.266	
0.27–0.43	"CH_2 stretch"	ν_{36}	0.358	ν_{36}	0.358	
		ν_{37}	0.362	ν_{37}	0.359	
		ν_{38}	0.363	ν_{38}	0.362	CH_2 stretch
		ν_{41}	0.370			
		ν_{44}	0.375	ν_{44}	0.376	
0.43–0.60	"OH stretch/ combination"	ν_{45}	0.455	ν_{45}	0.455	OH stretch
		$\nu_{18}+\nu_{37}$	0.491	$\nu_{18}+\nu_{37}$	0.488	
		$\nu_{18}+\nu_{38}$	0.492	$\nu_{18}+\nu_{38}$	0.491	Combination
		$\nu_{19}+\nu_{37}$	0.495	$\nu_{19}+\nu_{37}$	0.492	
		$\nu_{19}+\nu_{38}$	0.496	$\nu_{19}+\nu_{38}$	0.495	
0.60–0.80	"$2\times CH_2$ stretch"	$2\times\nu_{37}$	0.724	$2\times\nu_{37}$	0.718	
		$\nu_{37}+\nu_{38}$	0.725	$\nu_{37}+\nu_{38}$	0.721	$2\times CH_2$ stretch
		$2\times\nu_{38}$	0.726	$2\times\nu_{38}$	0.724	

[a]This vibrational frequency is comparable to our energy resolution so it may form combination bands that are unresolvable from the other fundamental vibrations.

detected energy loss between −0.2 and 0.8 eV. In this way the EELS are built up by continually scanning over the range of energy loss values, so that the effect of any minor variations in the target beam flux or incident electron current on an EELS is minimised. EELS at each E_0 and θ were repeatedly measured (2–4 times) to ensure reproducibility of the inelastic to elastic peak ratios (see later) within the experimental uncertainty.

As a part of this work, optimisation (and scaled[30]) frequency calculations were performed for the most abundant A and C conformers of THFA[11] at the B3LYP/aug-cc-pVDZ level in GAUSSIAN 09[31] with the results of those computations being given in Table I. This table shows the vibrational modes and combination bands of THFA with large infrared (IR) intensities. As noted previously, with an energy resolution of ∼65 meV many of those allowed modes overlap so that composite modes (see Table I) are experimentally assigned (see also Fig. 2). Note that many of these vibrations are similar to those observed in the energy loss assignments in Khakoo *et al.*[27] for THF. The respective EELS were now deconvoluted into contributions arising from each individual or unresolved combination of excited vibrational states. In each case one Gaussian function was used to describe the spectral profile for each resolvable inelastic feature and the elastic scattering peak, with typical examples of the results from those fits (in which the peak energies and peak widths are fixed in each case) being given in Fig. 2. The amplitudes of the Gaussian functions were then varied in a least-squares fitting procedure to provide the best fit to the measured spectra. The ratio (R) of the area under the fitting function for each ith vibrational feature to that under the elastic peak, at each E_0 and θ, is simply related to the ratio of the differential cross sections (σ) from:

$$R_i(E_0,\theta)=\frac{\sigma_i(E_0,\theta)}{\sigma_0(E_0,\theta)}. \quad (1)$$

Note that Eq. (1) is only valid if the transmission efficiency of the analyser remains constant over the energy loss and angular range studied, or is at least well characterised. Following a technique similar to that of Allan,[32] an additional focusing lens (synchronised to the voltage ramp) was also employed to minimise variations in the analyser transmission efficiency for electrons detected with different energy losses. Of course in these measurements the scattered electron energies are all very similar to that for E_0, so that a significant transmission effect would not be anticipated. Nonetheless, we place a conservative uncertainty of 20% on our

TABLE II. Present experimental vibrational-to-elastic ratios ($\times 10^{-3}$), differential cross sections ($\times 10^{-23}$ m^2/sr), and related uncertainty (%) for electron-impact vibrational excitation of the CC stretch in THFA (energy loss range 0.09–0.27 eV).

θ	20 eV			30 eV			40 eV			50 eV		
(deg)	Ratio	DCS	Uncertainty	Ratio	DCS	Uncertainty	Ratio	DCS	Uncertainty	Ratio	DCS	Uncertainty
10	6.22	420.48	29.4									
15	7.69	257.40	23.1	3.14	91.52	31.0	3.27	107.55	25.0	2.45	77.36	27.8
20	6.78	95.31	23.6	5.53	75.27	23.4	5.58	73.95	22.5	7.03	90.94	22.5
30	41.53	355.90	22.5	53.21	406.77	31.1	28.33	186.43	27.0	24.35	116.61	22.4
40	49.92	293.59	22.5	52.42	183.48	31.0	42.38	108.45	29.8	37.53	85.23	29.2
50	50.06	169.59	30.3	44.43	96.90	23.1	41.87	76.58	22.4	40.01	59.73	24.7
60	65.90	168.31	22.5	53.84	95.56	22.4	49.35	60.94	22.6	57.34	49.95	22.5
70	77.72	175.65	24.2	75.92	101.20	22.8	85.61	72.17	22.7	71.53	41.85	22.7
80	91.35	178.04	23.5	101.03	99.01	23.3	103.48	65.19	23.0	79.74	35.72	22.6
90	106.24	162.44	22.4	105.33	81.42	25.4	93.13	48.24	22.4	86.68	33.72	23.4

efficiency being unity. The present measured R_i for each of the "CC stretch," "CH_2 stretch," "OH stretch and combinations," and "2 × CH_2 stretch" are summarised in Tables II, III, IV, and V, respectively. It is immediately apparent from Eq. (1) that the product $R_i \times \sigma_0$ then gives the required composite vibrational mode DCS provided the elastic DCS (σ_0) is known. Those results, for the modes in question, can also be found in Tables II–V. In this study, we have utilised our IAM-SCAR elastic differential cross sections at 20, 30, 40, and 50 eV.[20] Note that no measured elastic DCSs for electron scattering from THFA, at energies below 50 eV, are currently published that we might compare the IAM-SCAR computations[20] against and thus possibly validate them. There is, however, a single elastic DCS measurement from Milosavljević *et al.*[16] at 50 eV, which is in fair accord[20] with our theoretical results at that energy. However, there are recent exemplars for elastic DCS of other species (e.g., Refs. 33–35) where our IAM-SCAR approach provides a good description of the measured cross sections down to 20 eV. There are also some cases[36,37] where the comparison between the IAM-SCAR elastic DCS and the measurements is only good at energies of ∼50 eV and above. Nonetheless, for the similar species THF, the IAM-SCAR method is found to be in good accord with available data,[13,38] at energies of ∼20 eV and above, and we are hopeful it will be similarly valid here.

The present vibrational excitation DCSs for the CC stretch, CH_2 stretch, OH stretch and combinations, and 2 × CH_2 stretch modes are respectively given in Tables II, III, IV, and V. Error estimates on those data are also given in each of these tables. Particular attention to the identification and quantification of all possible sources of error has been made throughout this study. In this case the statistical errors associated with the scattering intensity measurements are usually small (≤2%). An additional error due to our analyser transmission calibration (∼20%) must also be considered. While the inherent error in our IAM-SCAR elastic DCS computations, used in our normalisation, is negligible we have found from past experience[33–35,38] that it can often reproduce the experimental data to 10% or better. Hence, a 10% uncertainty on our elastic DCS has been incorporated into our analysis. Another important source of possible error is that associated with the numerical deconvolution of the energy loss spectra, so an allowance for this is also made in the overall DCS uncertainties. When all these factors are combined in quadrature, the errors on our DCS (see Tables II–V) are usually found to be in the range 22%–147%, with the largest errors only being for the 2 × CH_2 stretch mode for which the statistics were poorer due to its much smaller excitation probability (see Fig. 2). Our excitation DCSs, for each of the modes, are also plotted in Fig. 3.

TABLE III. Present experimental vibrational-to-elastic ratios ($\times 10^{-3}$), differential cross sections ($\times 10^{-23}$ m^2/sr), and related uncertainty (%) for electron-impact vibrational excitation of the CH_2 stretch in THFA (energy loss range 0.27–0.43 eV).

θ	20 eV			30 eV			40 eV			50 eV		
(deg)	Ratio	DCS	Uncertainty	Ratio	DCS	Uncertainty	Ratio	DCS	Uncertainty	Ratio	DCS	Uncertainty
10	1.05	70.70	23.8									
15	1.12	37.54	25.1	0.39	11.35	30.5	0.60	19.70	28.0	0.58	18.47	27.4
20	1.29	18.17	23.9	1.17	15.88	30.3	1.48	19.55	24.3	1.51	19.54	24.4
30	8.26	70.81	23.9	6.94	53.03	39.5	4.40	28.96	25.0	4.06	19.45	25.1
40	8.02	47.14	22.7	6.90	24.16	23.3	7.58	19.41	41.6	6.08	13.80	23.7
50	11.04	37.39	22.5	6.36	13.87	22.8	6.25	11.42	23.5	7.19	10.74	24.9
60	14.77	37.71	22.5	6.62	11.76	23.1	7.87	9.71	23.1	10.18	8.87	24.8
70	15.41	34.82	22.7	8.75	11.67	22.5	9.87	8.32	22.8	13.47	7.88	22.9
80	19.20	37.42	23.6	10.47	10.26	23.5	13.92	8.77	22.6	17.02	7.62	23.1
90	22.04	33.70	23.3	13.15	10.16	25.8	15.24	7.90	23.4	18.82	7.32	22.6

TABLE IV. Present experimental vibrational-to-elastic ratios ($\times 10^{-3}$), differential cross sections ($\times 10^{-23}$ m^2/sr), and related uncertainty (%) for electron-impact vibrational excitation of the OH stretch and combination modes in THFA (energy loss range 0.43–0.6 eV).

θ	20 eV			30 eV			40 eV			50 eV		
(deg)	Ratio	DCS	Uncertainty	Ratio	DCS	Uncertainty	Ratio	DCS	Uncertainty	Ratio	DCS	Uncertainty
10	0.23	15.49	40.1									
15	0.43	14.39	34.9	0.23	6.64	34.9	0.14	4.65	64.4	0.15	4.67	66.4
20	0.34	4.85	35.3	0.26	3.58	44.3	0.20	2.58	75.5	0.28	3.61	69.2
30	1.77	15.13	24.9	1.37	10.46	30.1	0.51	3.33	65.7	0.74	3.54	55.0
40	1.39	8.17	25.9	1.05	3.68	30.5	1.10	2.83	37.6	1.07	2.44	51.7
50	1.87	6.32	23.1	0.75	1.65	33.8	0.73	1.33	49.6	1.05	1.56	55.4
60	2.06	5.27	32.4	0.82	1.46	38.8	0.97	1.20	54.9	1.93	1.68	37.7
70	2.55	5.77	29.1	1.28	1.71	32.5	1.35	1.14	38.3	1.93	1.13	30.3
80	3.06	5.96	25.6	1.81	1.78	33.7	1.87	1.18	33.2	2.41	1.08	33.9
90	3.80	5.81	27.4	1.91	1.48	31.2	2.65	1.37	36.8	2.88	1.12	30.7

The DCS for a given scattering process, i, is related to the ICS, Q_i, through the standard formula:

$$Q_i(E_0) = 2\pi \int_0^{\pi} \sigma_i(E_0, \theta) \sin\theta d\theta. \quad (2)$$

In order to convert experimental DCS data, measured at discrete angles that span a finite angular range determined by the physical constraints of the apparatus, to an ICS, one must first extrapolate/interpolate the measured data so that it covers the full angular range from 0° to 180°. Our approach to accomplish this, built around a generalised oscillator strength formalism[39] for optically allowed states (we are dealing with a lot of infrared active modes here), has been discussed in great detail previously[40] and so we do not repeat that detail here. Rather, in Fig. 3(c) for the CC stretch mode, we indicate a representative result (shaded area) from our procedure. Note that while the 90°–180° extrapolation region is not specifically plotted, it contains no oscillating (unphysical) angular structure with a rather bland monotonic form in fact being found. Further note that this is also true for all our ICS analyses at each E_0 and for each vibrational excitation mode. The present ICSs, and the uncertainty on those data, are summarised in Table VI and plotted in Fig. 4. Note that the errors on our ICS, as well as incorporating those from the DCS (with allowance for the $\sin\theta$ weighting factor in Eq. (2)), also include an uncertainty in determining the extrapolation of our DCS to 0° and 180°. When these factors are accounted for, the ICS errors are found to be in the range 43%–99%with the precise error depending on the energy and vibrational mode in question.

III. RESULTS AND DISCUSSION

In Tables II–V and Fig. 3 we present the differential cross section results, for electron impact excitation of the CC stretch, CH_2 stretch, OH stretch plus combination, and $2 \times CH_2$ stretch modes in THFA, from our experimental investigations. In Fig. 3(a) we also plot corresponding vibrational excitation results on THF from Khakoo *et al.*[27] In addition, our derived integral cross section results are given in Table VI and plotted in Fig. 4, where they are again compared to the relevant THF results.[27] Note that in Table VI we also list the summed integral cross section values for all the modes identified in the 0.09–0.8 eV energy loss range, with that data being plotted and compared to the THF ICS sum in Fig. 5. All the errors listed in Tables II–VI and plotted in Figs. 3–5 are at the one standard deviation level.

Let us consider Fig. 3 in more detail. Here, we observe that for each energy and for each composite excitation mode, the angular distributions display no forward peaking

TABLE V. Present experimental vibrational-to-elastic ratios ($\times 10^{-3}$), differential cross sections ($\times 10^{-23}$ m^2/sr), and related uncertainty (%) for electron-impact vibrational excitation of the $2 \times CH_2$ stretch in THFA (energy loss range 0.6–0.8 eV).

θ	20 eV			30 eV			40 eV			50 eV		
(deg)	Ratio	DCS	Uncertainty	Ratio	DCS	Uncertainty	Ratio	DCS	Uncertainty	Ratio	DCS	Uncertainty
10	0.10	6.71	62.0									
15	0.14	4.53	88.6	0.10	2.87	66.8	0.06	2.04	138.3	0.06	2.02	146.1
20	0.21	3.01	47.8	0.13	1.74	75.1	0.11	1.52	122.6	0.14	1.86	114.1
30	1.06	9.09	27.1	0.44	3.34	59.9	0.27	1.79	115.3	0.16	0.75	253.2
40	0.99	5.85	28.1	0.32	1.10	67.2	0.34	0.87	89.3	0.36	0.82	136.4
50	1.27	4.29	24.3	0.49	1.07	47.3	0.30	0.55	110.7	0.35	0.53	147.0
60	1.67	4.27	33.2	0.54	0.95	52.7	0.28	0.34	160.2	0.82	0.71	86.4
70	1.90	4.29	31.4	0.80	1.07	43.1	0.59	0.50	75.1	0.56	0.33	75.9
80	2.11	4.11	29.2	1.04	1.02	41.2	0.63	0.40	59.8	0.85	0.38	75.8
90	2.17	3.32	30.2	1.06	0.82	40.7	0.77	0.40	74.6	1.01	0.39	63.6

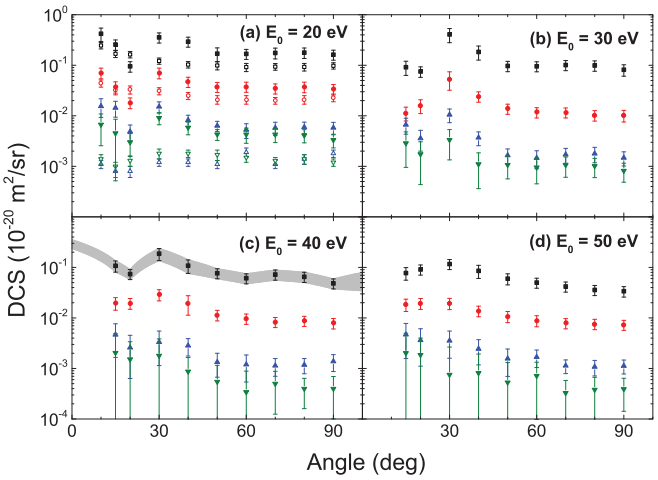

FIG. 3. Differential cross sections ($\times 10^{-20}$ m^2/sr) for vibrational excitation of THFA at various incident electron energies: (a) 20 eV, (b) 30 eV, (c) 40 eV, and (d) 50 eV. Shown are the DCSs for the four vibrational features: (■) predominantly CC stretch (energy loss range 0.09–0.27 eV), (●) CH_2 stretch (0.27–0.43 eV), (▲) OH stretch plus combination band (0.43–0.6 eV); (▼) 2 × CH_2 stretch (0.6–0.8 eV). Also plotted in (a) are the DCSs for vibrational excitation of THF by Khakoo *et al.*[27] for various excitation energy ranges: (□) 0.084–0.261 eV, predominantly CC stretch; (○) 0.262–0.444 eV, mostly CH_2 stretch; (△) 0.445–0.616 eV, combination modes; (▽) 0.617–0.796 eV, 2 × CH_2 stretch. Also shown in (c) is an example of the extrapolation and interpolation of the DCS for the CC stretch mode, that was used to determine the ICS (see text for further details).

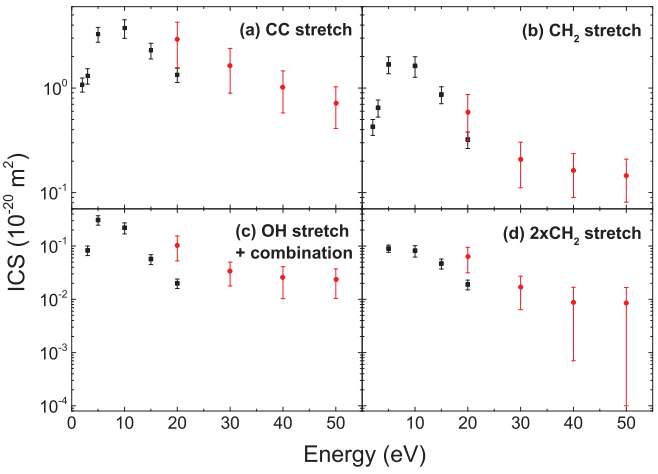

FIG. 4. Integral cross sections ($\times 10^{-20}$ m^2) for vibrational excitation of THFA (●) as a function of the incident electron energy for various vibrational modes: (a) mostly CC stretch (energy loss range 0.09–0.27 eV), (b) CH_2 stretch (0.27–0.43 eV), (c) OH stretch plus combination bands (0.43–0.6 eV), (d) 2 × CH_2 stretch (0.6–0.8 eV). Also plotted are the ICSs for vibrational excitation of THF (■) by Khakoo *et al.*[27] for similar excitation energy ranges: (a) 0.084–0.261 eV, predominantly CC stretch; (b) 0.262–0.444 eV, mostly CH_2 stretch; (c) 0.445–0.616 eV, combination modes; (d) 0.617–0.796 eV, 2 × CH_2 stretch.

in the magnitude of their cross sections. Indeed, while there is a suggestion of some small "structure" associated with those angular distributions, to within the errors on the DCSs their shapes are almost quasi-isotropic over the angular range considered. We had not anticipated this result, given that in our electronic-state excitation studies all the THFA measured DCSs were very strongly peaked in magnitude at forward scattering angles.[20,41] Note that this behaviour in the excitation cross sections of the electronic-states in THFA was attributed to the strong dipole scattering effect on the collision dynamics. Therefore, should we conclude here that the absence of this forward peaking in the vibrational excitation angular distributions is indicative for the permanent dipole moment and/or dipole polarisability of THFA not being important, for some reason, in the excitation of its vibrational modes? Before considering that question, let us note that the behaviour observed in Fig. 3 for THFA is certainly not unique. Khakoo *et al.*,[27] for electron energies in the range 3–20 eV, found a very similar effect in THF (a polar cyclic ether like THFA). Similarly, from that same group, in an earlier study of vibrational excitation in furan, Hargreaves *et al.*[42] again observed quasi-isotropic angular distributions. If we now focus on Fig. 3(a), our results at 20 eV, then we can compare the present THFA results to those for THF from Khakoo *et al.*[27] While for each mode the shapes of the THFA and THF differential cross sections are quite similar, the present THFA DCSs are systematically larger in absolute value compared to those of THF. As the permanent dipole moment of THF is ∼1.63 D,[43] very similar to that for THFA given earlier, it is probably reasonable to suppose that any effect it might have on the vibrational excitation process could be similar in both species. On the other hand the dipole polarisability of THF is only ∼47.08 a.u.,[44] which is rather smaller than that of THFA. Therefore one possibility to explain the observed mismatch in absolute value, for the corresponding composite vibrational modes, between THFA and THF, might be the stronger dipole polarisability of THFA vis-à-vis THF. Note that if we accept this hypothesis, then the answer to the question we posed above is that at least the dipole polarisability, which represents the response of the molecular charge cloud to the incident projectile electron, might be having an effect

TABLE VI. Present experimental integral cross sections ($\times 10^{-22}$ m^2) and related uncertainty (%) for electron-impact excitation of the vibrational features in THFA.

	20 eV		30 eV		40 eV		50 eV	
Feature	ICS	Uncertainty	ICS	Uncertainty	ICS	Uncertainty	ICS	Uncertainty
CC stretch	291.45	46.2	164.60	45.7	101.75	43.2	71.87	42.9
CH_2 stretch	59.12	46.6	20.76	46.3	16.31	44.9	14.51	44.2
OH stretch + combination	10.37	49.1	3.39	47.5	2.56	59.8	2.38	56.3
2 × CH_2 stretch	6.31	50.2	1.68	61.9	0.88	92.0	0.84	98.8
Sum	367.25	37.5	190.43	39.8	121.5	36.7	89.6	35.2

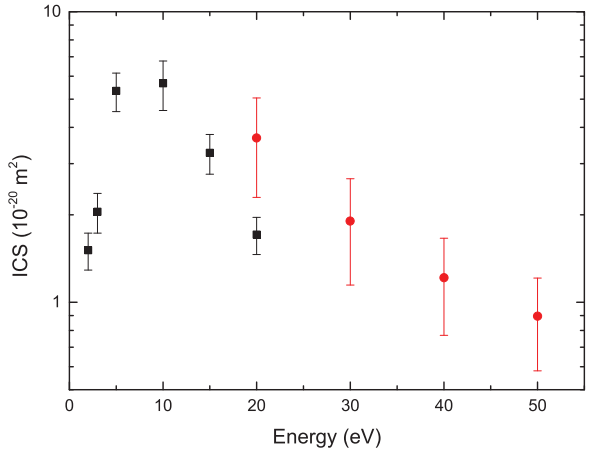

FIG. 5. Integral cross sections ($\times 10^{-20}$ m^2) for the summed vibrational excitations of THFA (●), in the energy loss range 0.09–0.8 eV, as a function of the incident electron energy. Also plotted are the ICSs for the summed vibrational excitations of THF (■) by Khakoo *et al.*[27]

on the vibrational excitation collision dynamics. However another plausible explanation for this difference in the THFA versus THF mismatch in absolute magnitude, might relate to a difference in their respective density of states in the relevant energy loss regions. Specifically, while THF has 33 vibrational modes THFA has 45 with some of those extra modes of THFA greatly enhancing its IR activity particularly in the CC-stretch region. Hence it is possible that it is these additional vibrations in THFA that are causing its cross sections to be somewhat larger in magnitude than those for THF.

Perhaps this same latter point is made more apparent by considering Figs. 4 and 5, the integral cross sections for excitation of the THFA and THF[27] composite modes and their sums, respectively. In this case we can plot all the Khakoo *et al.* ICS data from 2 − 20 eV, and compare that to the present 20 − 50 eV ICS. The trend in this comparison, from Fig. 4, is that our THFA ICSs are uniformly stronger in magnitude compared to those of THF for each mode. Note that while the errors we have cited on our ICS might be on the conservative side, we suspect the errors cited by Khakoo *et al.* are somewhat optimistic. Nonetheless, this point does not affect our above observation. While no real energy-dependent structure is apparent in any of our vibrational ICS in Fig. 4, this is not surprising as the TCS data for THFA[15] only shows the existence of important shape resonance effects at somewhat lower energies. On the other hand, for THF, the well-known shape resonance[45] is observed in most of their[27] composite vibrational mode cross sections. If we consider the magnitudes of the Khakoo *et al.* data,[27] near the peaks in the resonance enhanced cross sections (see Fig. 4) and use proposed values for the elastic ICS of THF, in this same energy region, that are available in the literature,[5,13] then it is clear that at resonance the vibrational modes of THF are making a quite significant contribution to the THF total cross section. Given the many similar physico-chemical features between THFA and THF, such an effect in resonant vibrational excitation of THF might also be seen in THFA near its shape resonances.[15] We believe this certainly warrants further investigation. A similar story to that just described in Fig. 4, is also found in Fig. 5 for the summed ICS. Nonetheless, it is perhaps instructive to compare the value of our THFA 20 eV summed ICS divided by that for THF at 20 eV to the ratio of the dipole polarisabilities of THFA and THF. On doing so we find a cross section ratio of 2.15 ± 0.86, while the ratio of the dipole polarisabilities is 1.49. Thus the two ratios are consistent to within the uncertainty. While we cannot rule out that the level of agreement between these ratios is something of a coincidence, it may also provide some further evidence in support of the notion that the dipole polarisability is playing a role in the electron impact vibrational excitation of THF.

IV. CONCLUSIONS

We have reported on differential and integral cross section measurements for excitation of a number of composite vibrational modes in α-tetrahydrofurfuryl alcohol, in the energy range 20–50 eV. To the best of our knowledge, no other theoretical or experimental data are currently available in the literature to compare against the present results. While the angular distributions of our vibrational DCSs were largely quasi-isotropic, an argument for why the dipole polarisability of THFA might still be influencing the vibrational excitation process was advanced. However, as we also noted, the observed THFA versus THF cross section behaviour might also be understood on the basis of a density of states argument. A clear need for theoretical calculations to help elucidate the important factors driving the collision dynamics of this scattering system is apparent, although we do not underestimate the difficulties of such computations. Finally, an extension of the present measurements, although probably employing excitation functions (DCS versus energy at a given θ) rather than our approach here, to the energy region where shape resonances in the THFA total cross section[15] are known, we believe would be interesting and beneficial.

ACKNOWLEDGMENTS

The authors wish to thank the Australian (through the Australian Research Council), Brazilian (through CNPq and FAPEMIG), Portuguese (PEst-OE/FIS/UI0068/2014 and PTDC/FIS-ATO/1832/2012 through FCT-MEC), and Spanish (Ministerio de Economia y Competitividad under Project FIS2012-31230) funding agencies who financially supported various aspects of this work. One of us (M.J.B.) acknowledges the University of Malaya for his "Distinguished Visiting Professor" appointment and CNPq for his "Special Visiting Professorship," while another (D.B.J.) thanks the ARC for his Discovery Early Career Research Award. Finally, H.V.D. thanks the "Science Without Borders" scheme that enabled him to visit and study in Australia.

[1] M. J. Brunger and S. J. Buckman, Phys. Rep. **357**, 215 (2002).
[2] J.-S. Yoon, M.-Y. Song, H. Kato, M. Hoshino, H. Tanaka, M. J. Brunger, S. J. Buckman, and H. Cho, J. Phys. Chem. Ref. Data **39**, 033106 (2010).
[3] L. Campbell and M. J. Brunger, Plasma Sources Sci. Technol. **22**, 013002 (2013).
[4] K. F. Ness, R. E. Robson, M. J. Brunger, and R. D. White, J. Chem. Phys. **136**, 024318 (2012).

[5]N. A. Garland, M. J. Brunger, G. Garcia, J. de Urquijo, and R. D. White, Phys. Rev. A **88**, 062712 (2013).
[6]A. G. Sanz, M. C. Fuss, A. Muñoz, F. Blanco, P. Limão-Vieira, M. J. Brunger, S. J. Buckman, and G. García, Int. J. Radiat. Biol. **88**, 71 (2012).
[7]Z. Lj. Petrović, S. Marjanović, S. Dujko, A. Banković, G. Malović, S. Buckman, G. Garcia, R. White, and M. Brunger, Appl. Radiat. Isot. **83**, 148 (2014).
[8]R. D. White, W. Tattersall, G. Boyle, R. E. Robson, S. Dujko, Z. Lj. Petrovic, A. Bankovic, M. J. Brunger, J. P. Sullivan, S. J. Buckman, and G. Garcia, Appl. Radiat. Isot. **83**, 77 (2014).
[9]L. Campbell, M. J. Brunger, Z. L. Petrovic, M. Jelisavcic, R. Panajotovic, and S. J. Buckman, Geophys. Res. Lett. **31**, L10103, doi:10.1029/2003GL019151 (2004).
[10]R. D. White, M. J. Brunger, N. A. Garland, R. E. Robson, K. F. Ness, G. García, J. de Urquijo, S. Dujko, and Z. Lj. Petrović, Eur. Phys. J. D **68**, 125 (2014).
[11]P. Limão-Vieira, D. Duflot, M.-J. Hubin-Franskin, J. Delwiche, S. V. Hoffmann, L. Chiari, D. B. Jones, M. J. Brunger, and M. C. A. Lopes, "Electronic states of tetrahydrofurfuryl alcohol (THFA) as studied by VUV spectroscopy and *ab initio* calculations," J. Phys. Chem. A (published online, 2014).
[12]H. V. Duque, L. Chiari, D. B. Jones, P. A. Thorn, Z. Pettifer, G. B. da Silva, P. Limão-Vieira, D. Duflot, M.-J. Hubin-Franskin, J. Delwiche, F. Blanco, G. García, M. C. A. Lopes, K. Ratnavelu, R. D. White, and M. J. Brunger, "Cross sections for electron scattering from α-tetrahydrofurfuryl alcohol," Chem. Phys. Lett. (in press).
[13]M. Fuss, A. G. Sanz, F. Blanco, P. Limão-Vieira, M. J. Brunger, and G. García, "Differential and integral electron scattering cross sections from tetrahydrofuran (THF) over a wide energy range: 1-10000 eV," Eur. Phys. J. D (in press).
[14]P. Możejko and L. Sanche, Radiat. Phys. Chem. **73**, 77 (2005).
[15]P. Możejko, A. Domaracka, E. Ptasińska-Denga, and C. Szmytkowski, Chem. Phys. Lett. **429**, 378 (2006).
[16]A. R. Milosavljević, F. Blanco, D. Šević, G. García, and B. P. Marinković, Eur. Phys. J. D **40**, 107 (2006).
[17]A. R. Milosavljević, J. Kocisek, P. Papp, D. Kubala, B. P. Marinković, P. Mach, J. Urban, and S. Matejcik, J. Chem. Phys. **132**, 104308 (2010).
[18]S. M. Bellm, J. D. Builth-Williams, D. B. Jones, H. Chaluvadi, D. H. Madison, C. G. Ning, F. Wang, X. Ma, B. Lohmann, and M. J. Brunger, J. Chem. Phys. **136**, 244301 (2012).
[19]D. B. Jones, J. D. Builth-Williams, S. M. Bellm, L. Chiari, H. Chaluvadi, D. H. Madison, C. G. Ning, B. Lohmann, O. Ingólfsson, and M. J. Brunger, Chem. Phys. Lett. **572**, 32 (2013).
[20]L. Chiari, H. V. Duque, D. B. Jones, Z. Pettifer, G. B. da Silva, P. Limão-Vieira, D. Duflot, M.-J. Hubin-Franskin, J. Delwiche, G. García, F. Blanco, M. C. A. Lopes, K. Ratnavelu, R. D. White, and M. J. Brunger, "Differential cross sections for intermediate-energy electron scattering from α-tetrahydrofurfuryl alcohol: excitation of electronic-states," J. Chem. Phys. (submitted).
[21]A. Zecca, L. Chiari, G. Garciá, F. Blanco, E. Trainotti, and M. J. Brunger, New J. Phys. **13**, 063019 (2011).
[22]B. C. Ibanescu, O. May, A. Monney, and M. Allan, Phys. Chem. Chem. Phys. **9**, 3163 (2007).
[23]C. Szmytkowski and E. Ptasińska-Denga, J. Phys. B **44**, 015203 (2011).
[24]M. J. Brunger, L. Campbell, D. C. Cartwright, A. G. Middleton, B. Mojarrabi, and P. J. O. Teubner, J. Phys. B **33**, 783 (2000).
[25]H. Kato, H. Kawahara, M. Hoshino, H. Tanaka, M. J. Brunger, and Y.-K. Kim, J. Chem. Phys. **126**, 064307 (2007).
[26]H. Kato, M. Hoshino, H. Tanaka, P. Limão-Vieira, O. Ingólfsson, L. Campbell, and M. J. Brunger, J. Chem. Phys. **134**, 134308 (2011).
[27]M. A. Khakoo, D. Orton, L. R. Hargreaves, and N. Meyer, Phys. Rev. A **88**, 012705 (2013).
[28]T. P. T. Do, M. Leung, M. Fuss, G. Garcia, F. Blanco, K. Ratnavelu, and M. J. Brunger, J. Chem. Phys. **134**, 144302 (2011).
[29]M. J. Brunger and P. J. O. Teubner, Phys. Rev. A **41**, 1413 (1990).
[30]*NIST Computational Chemistry Comparison and Benchmark Database*, NIST Standard Reference Database Number 101, Release 16a, August 2013, edited by R. D. Johnson III (see http://cccbdb.nist.gov/).
[31]M. J. Frisch, G. W. Trucks, H. B. Schlegel *et al.*, GAUSSIAN 09, Revision B.01, Gaussian Inc., Wallingford, CT, 2010.
[32]M. Allan, J. Phys. B **38**, 3655 (2005).
[33]H. Kato, A. Suga, M. Hoshino, F. Blanco, G. García, P. Limão-Vieira, M. J. Brunger, and H. Tanaka, J. Chem. Phys. **136**, 134313 (2012).
[34]H. Kato, K. Anzai, T. Ishihara, M. Hoshino, F. Blanco, G. García, P. Limão-Vieira, M. J. Brunger, S. J. Buckman, and H. Tanaka, J. Phys. B **45**, 095204 (2012).
[35]H. Murai, Y. Ishijima, T. Mitsumura, Y. Sakamoto, H. Kato, M. Hoshino, F. Blanco, G. García, P. Limão-Vieira, M. J. Brunger, S. J. Buckman, and H. Tanaka, J. Chem. Phys. **138**, 054302 (2013).
[36]J. R. Brunton, L. R. Hargreaves, S. J. Buckman, G. García, F. Blanco, O. Zatsarinny, K. Bartschat, and M. J. Brunger, Chem. Phys. Lett. **568–569**, 55 (2013).
[37]P. Palihawadana, J. P. Sullivan, S. J. Buckman, Z. Mašín, J. D. Gorfinkiel, F. Blanco, G. García, and M. J. Brunger, J. Chem. Phys. **139**, 014308 (2013).
[38]M. Fuss, A. Muñoz, J. C. Oller, F. Blanco, D. Almeida, P. Limão-Vieira, T. P. D. Do, M. J. Brunger, and G. García, Phys. Rev. A **80**, 052709 (2009).
[39]E. N. Lassettre, J. Chem. Phys. **43**, 4479 (1965).
[40]Z. Mašín, J. D. Gorfinkiel, D. B. Jones, S. M. Bellm, and M. J. Brunger, J. Chem. Phys. **136**, 144310 (2012).
[41]M. J. Brunger, S. J. Buckman, J. P. Sullivan, P. Palihawadana, D. B. Jones, L. Chiari, Z. Pettifer, G. B. da Silva, M. C. A. Lopes, H. V. Duque, Z. Mašín, J. D. Gorfinkiel, G. García, M. Hoshino, H. Tanaka, and P. Limão-Vieira, AIP Conf. Proc. **1588**, 71 (2014).
[42]L. R. Hargreaves, R. Albaridy, G. Serna, M. C. A. Lopes, and M. A. Khakoo, Phys. Rev. A **84**, 062705 (2011).
[43]D. Bouchiha, J. D. Gorfinkiel, L. G. Caron, and L. Sanche, J. Phys. B **40**, 1259 (2007).
[44]A. Zecca, L. Chiari, A. Sarkar, and M. J. Brunger, J. Phys. B **41**, 085201 (2008).
[45]M. Allan, J. Phys. B **40**, 3531 (2007).
[46]S. M. Kerwin, J. Am. Chem. Soc. **132**, 2466 (2010).